Supplementary Information for

Thin Film of Sulfonated Zinc Phthalocyanine/Layered Double Hydroxide for Achieving Multiple Quantum Well Structure and Polarized Luminescence

Dongpeng Yan,[a] Shenghui Qin,[a] Li Chen,[a] Jun Lu, [a*] Jing Ma,[b] Min Wei,[a*] David G. Evans,[a] and Xue Duan[a]

[a] *State Key Laboratory of Chemical Resource Engineering, Beijing University of Chemical Technology, Beijing 100029, P. R. China.*

[b] *School of chemistry and chemical engineering, Key Laboratory of Mesoscopic Chemistry of MOE, Nanjing University, Nanjing, 210093, P.R. China.*

List of Contents

1. Experimental details for (ZnTSPc/LDH)$_n$ TFs.

1.1 Reagents and materials: Zinc tetrasulfophthalocyanine tetrasodium salt ($Na_4ZnTSPc$) was purchased from Sigma Chemical. Co. Ltd. Analytical grade $Mg(NO_3)_2{\cdot}6H_2O$, Al $(NO_3)_3{\cdot}9H_2O$ and urea were purchased from Beijing Chemical Co. Ltd. and used without further purification.

1.2 Fabrication of (ZnTSPc/LDH)$_n$ and pristine ZnTSPc TFs: The processes of synthesis and exfoliation of Mg-Al-LDH were similar to that described in our previous work.[1a] 0.1 g of Mg-Al-LDH was shaken in 100 cm^3 of formamide for 24 h to produce a colloidal suspension of exfoliated Mg-Al-LDH nanosheets. The quartz glass substrate was cleaned in concentrated NH_3/30% H_2O_2 (7:3) and concentrated H_2SO_4 for 30 min each. After each procedure, the quartz substrate was washed thoroughly with deionic water. The substrate was dipped in a colloidal suspension (1 g $\cdot L^{-1}$) of LDH nanosheets for 10 min followed by washing thoroughly, and then the substrate was treated with a 100 mL of ZnTSPc aqueous solution (1 mmol/L) for 10 min. The multilayer (ZnTSPc/LDH)$_n$ TFs were fabricated by alternate deposition of LDH nanosheets suspension and ZnTSPc solution for *n* cycles. The resulting films were dried under a nitrogen gas flow for 2 min at 20 °C. The EDX present the relative percentage content of the element in the $(ZnTSPc/LDH)_{32}$ film: Mg: 12.13%; Al: 7.26%; Zn: 3.87%; C: 23.19%; O: 40.11%; S: 7.51%. The real composition for the thin film can be expressed as: $Mg_{1.958}Al_{1.042}(OH)_6[(C_{32}H_{16}N_8O_{12}S_4Zn)_{0.230}][(CO_3)_{0.061}]$. The pristine ZnTSPc film was fabricated by the solvent evaporation method; a solution of ZnTSPc in ethanol (10^{-5} M) was thoroughly dispersed under ultrasonic and then extended on a quartz substrate that was fully cleaned by an ultrasonic anhydrous ethanol bath.

1.3 Sample characterization: The UV-vis absorption spectra were collected in the range from 300 to 900 nm on a Shimadzu U-3000 spectrophotometer, with the slit width of 1.0 nm. The fluorescence spectra were performed on RF-5301PC fluorospectrophotometer with the excitation wavelength of 610 nm, and both the excitation and emission slit were set to 10 nm. The incident and emissive light direction is 45 degree respective to the film, respectively. Steady-state polarized photoluminescence measurements of ZnTSPc/LDH TFs were recorded with an Edinburgh Instruments' FLS 920 fluorospectrophotometer. X-ray diffraction patterns (XRD) of ZnTSPC/LDH TFs were recorded using a Rigaku 2500VB2+PC diffractometer under the conditions: 40 kV, 50 mA, Cu Kα radiation (λ = 0.154056 nm) with step-scanned in step of 0.04° (2θ) in the range from 3 to 10° using a count time of 10 s/step. The morphology of thin films was investigated by using a scanning electron

microscope (SEM Hitachi S-3500) equipped with an EDX attachment (EDX Oxford Instrument Isis 300), and the accelerating voltage applied was 20 kV. The surface roughness and thickness data were obtained by using the atomic force microscopy (AFM) software (Digital Instruments, Version 6.12).

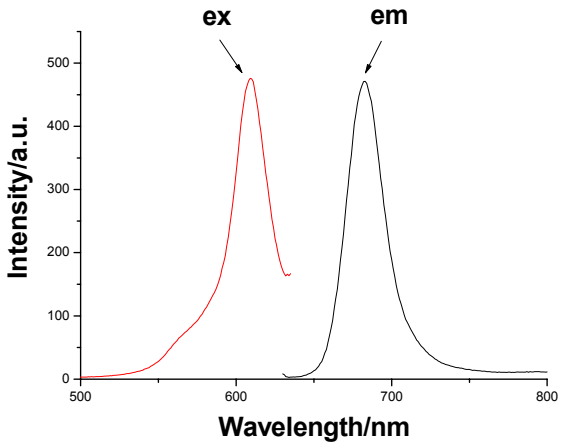

Fig. S1. Excitation and emission spectra of ZnTSPc in aqueous solution (10 μM).

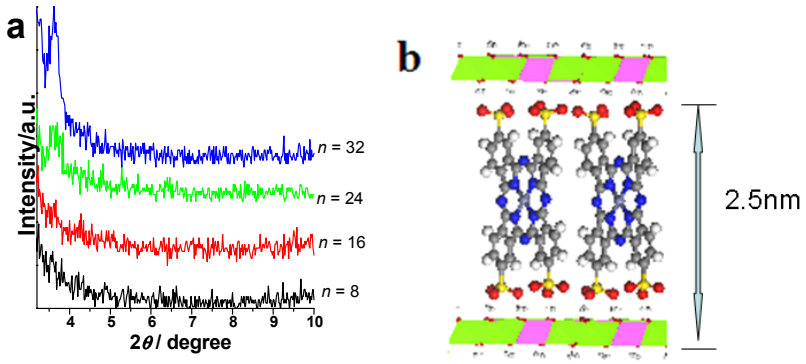

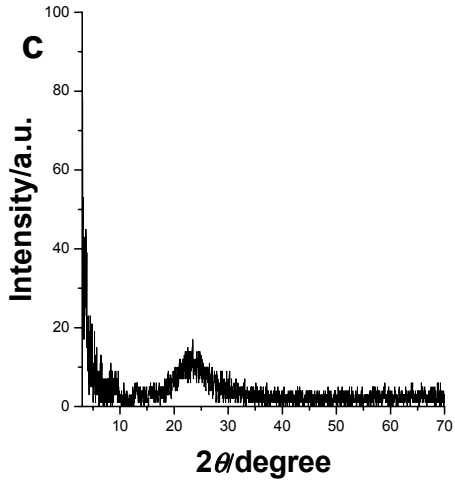

Fig. S2. (a) The small angle XRD profiles for the $(ZnTSPc/LDH)_n$ TFs with 8, 16, 24, 32 bilayers; (b) The structural model of ZnTSPc/LDH. (c) The XRD profile for $(ZnTSPc/LDH)_{32}$ in the range 3-70°. It can be speculated from the XRD observation that the ZnTSPc exhibit perpendicular to the LDH layers, which is similar to that of the Cu-Pc intercalated LDH system.[1b] It can also be observed that except for a broad band in the range 20-30° (the amorphous diffraction peak of the quartz substrate), there is no other peaks can be observed.

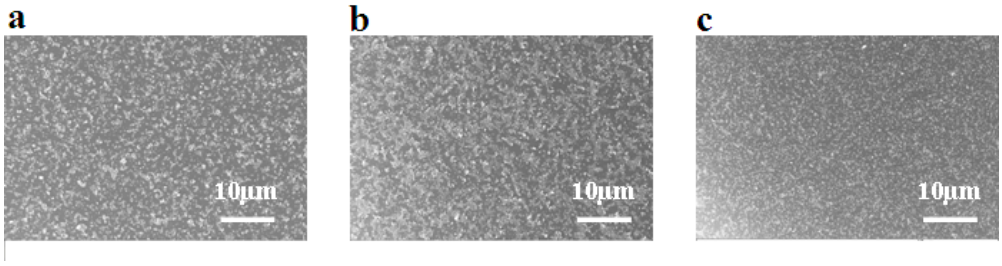

Fig. S3. The top view of SEM images for the $(ZnTSPc/LDH)_n$ TFs with a) 8, b)16, c) 24 bilayers.

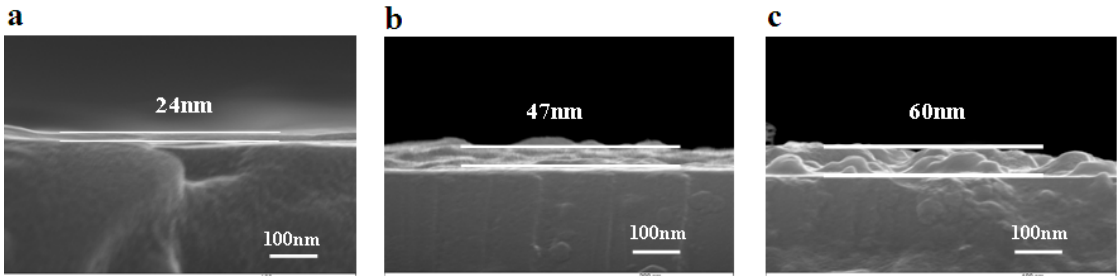

Fig. S4. The side view of SEM images for the $(ZnTSPc/LDH)_n$ TFs with a) 8, b) 16, c) 24 bilayers.

Table S1: The depth and thickness parameters for the TFs with 8, 16, 24, 32 bilayers

n	**8**	**16**	**24**	**32**
rms roughness (nm)[a]	6.175	8.034	11.045	13.737

SEM thickness (nm)[b]	*ca*. 24	*ca*. 47	*ca*. 60	*ca*. 83

[a] The values of statistical rms roughness were obtained by AFM.

[b] The SEM thickness were obtained from the side view of $(ZnTSPc/LDH)_n$ TFs, see Fig. S4.

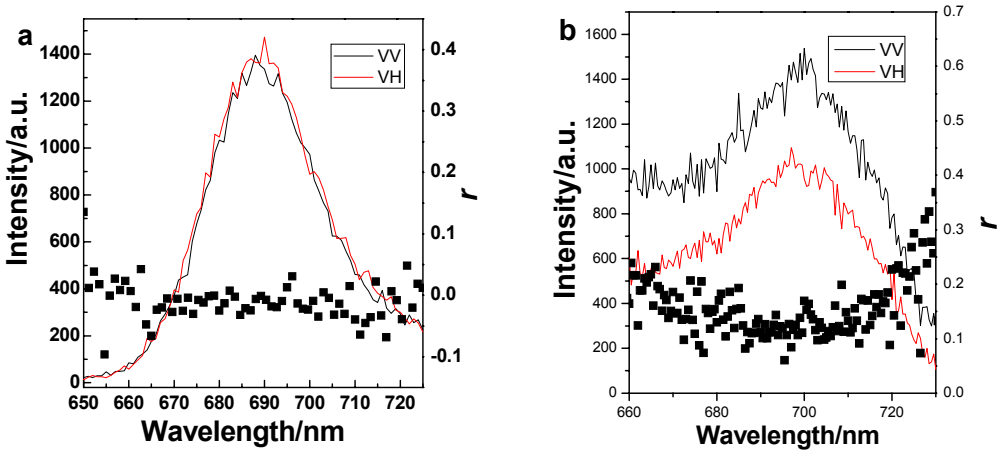

Fig. S5. Polarized fluorescence profiles for the VV, VH modes and anisotropic value (*r*) for a). the ZnTSPc solution (10 μM) and b). the pristine ZnTSPc film.

2. Calculation details and analysis of $(ZnTSPc/LDH)_n$ TFs.

Building of the structural model of ZnTSPc/LDH system and computational method: An ideal LDH layer with R3-m space group containing 8 Mg atoms and 4 Al atoms was built. The lattice parameters of the 2-dimensional layer are $a = b = 3.05$ Å, which is in accordance with other literatures.[2] Every octahedral layer has 12 metal atoms and 24 OH groups, and a supercell was constructed with lattice parameter a =10.57 Å, b = 9.15 Å and the initial interlayer spacing c = 25 Å, $\alpha = \beta = \gamma = 90°$. The supercell was treated as P1 symmetry, and a three-dimensional periodic boundary condition was applied. Then the ZnTSPc ($C_{32}H_{16}N_8O_{12}S_4Zn^{4-}$) with four negative charges was introduced into the simulated supercell, in which the sulfonate groups are normal to the LDH layer as the initial configuration. As a result, the formula of the simulated structure can be expressed as: $Mg_8Al_4(OH)_{24}(C_{32}H_{16}N_8O_{12}S_4Zn)$. All calculations were performed with the periodic density functional theory (DFT) method using Dmol3[3a,b] module in Material Studio software package.[4c] The initial configuration was first fully optimized with fixed positions for the atoms in the layer by

classical molecular mechanics method employed cff91 force field,[3d-f] and then further optimization was implemented by both Perdew-Wang (PW91)[3g] generalized gradient approximation (GGA) and Vosko–Wilk–Nusair (VWN)[3h] local-density approximation (LDA) methods with the double numerical basis sets plus polarization function (DNP). The core electrons for metals were treated by effective core potentials (ECP). SCF converged criterion was within 1.0×10^{-5} hartree/atom and converged criterion of structure optimization was 1.0×10^{-3} hartree/bohr. The Brillouin zone is sampled by 1×1×1 *k*-points, and test calculations reveal that the increase of *k*-points does not affect the results.

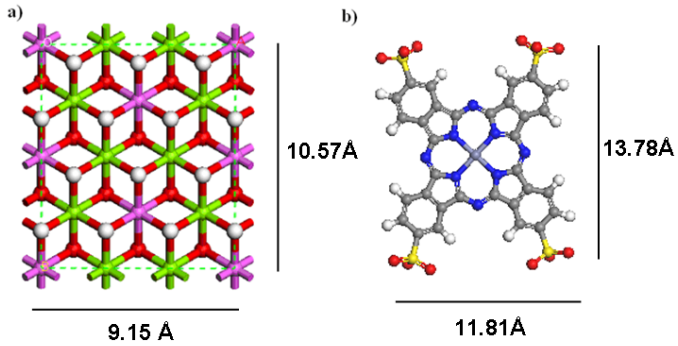

Fig. S6. a) The tetragonal superlattice model for Mg-Al-LDH layer (Color codes: white: H; red: O; pink: Al; green: Mg); b) the structural model of ZnTSPc $(C_{32}H_{16}N_8O_{12}S_4Zn)^{4-}$.

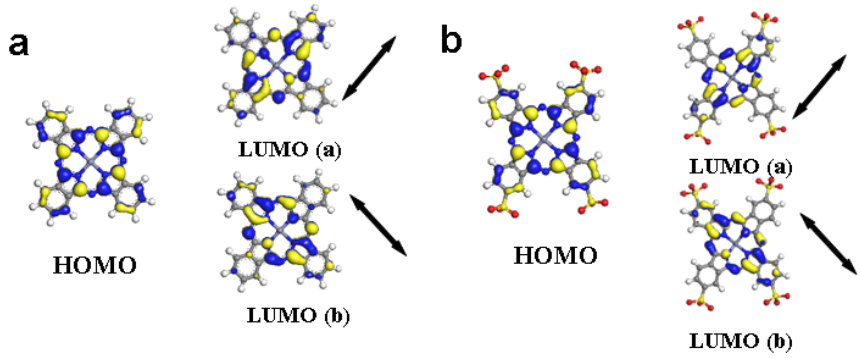

Fig. S7. The typical HOMO and LUMO profiles calculated by the VMN functional for a) the pristine ZnPc and b) the pristine ZnTSPc. The arrows show the direction of the transition dipole moment of the ZnPc and ZnTSPc.

For the zinc phthalocyanine (ZnPc) and ZnTSPc molecules, it can be observed from Fig. S7 that the HOMOs are mainly distributed on the C atoms of the heterocyclic ring and phenyl ring in ZnTSPc; the LUMOs, comprised of two degeneration orbitals, are mainly located on the C and N

atoms in the heterocyclic ring. The results demonstrate that the sulfonate group does not influence the excitation and emission processes of the ZnTSPc. The DFT results in this work are well consistent with that of Morley's work[4a] calculated by the combination of the AM1 and CNDO/S method.

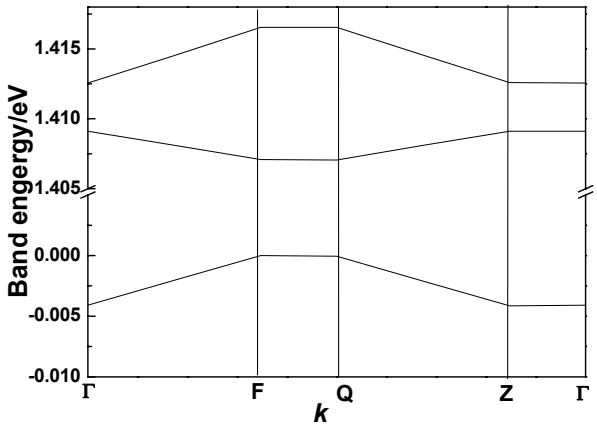

Fig. S8. a) A typical calculated band structure around the Fermi energy level of ZnTSPc/LDH system calculated by the VMN functional. Γ(0,0,0), Z (0,0,1/2), F (0,1/2,0), and Q (1/2,0,0) are the selected reciprocal points in the first Brillouin Zone (BZ). The energy gap between conduction band (CB) and valance band (VB) at Γ point (0,0,0) in the first BZ is 1.41 eV.

The energy bands around the Fermi levels show independence on the *k* electron wave vectors along the ΓZ line ([001] direction), indicating the strong valence electron confinement effect of the LDH monolayer in the normal direction.

Table S2: The calculated band gap energy of the ZnPc, ZnTSPc and ZnTSPc/LDH

Band energy (eV)	ZnPc	ZnTSPc	ZnTSPc/LDH
VMN-LDA	1.45	1.42	1.41
PW91-GGA	1.43	1.41	1.38

The band gap of the ZnPc calculated by both methods mentioned above is lower than that of Liao's work (1.91eV);[4b] whereas the results are very close to the other M-Pc systems: Fe-Pc (1.38 eV); Ni-Pc (1.47 eV); Cu-Pc (1.42 eV); Mg-Pc (1.38 eV) in literature.[4b]

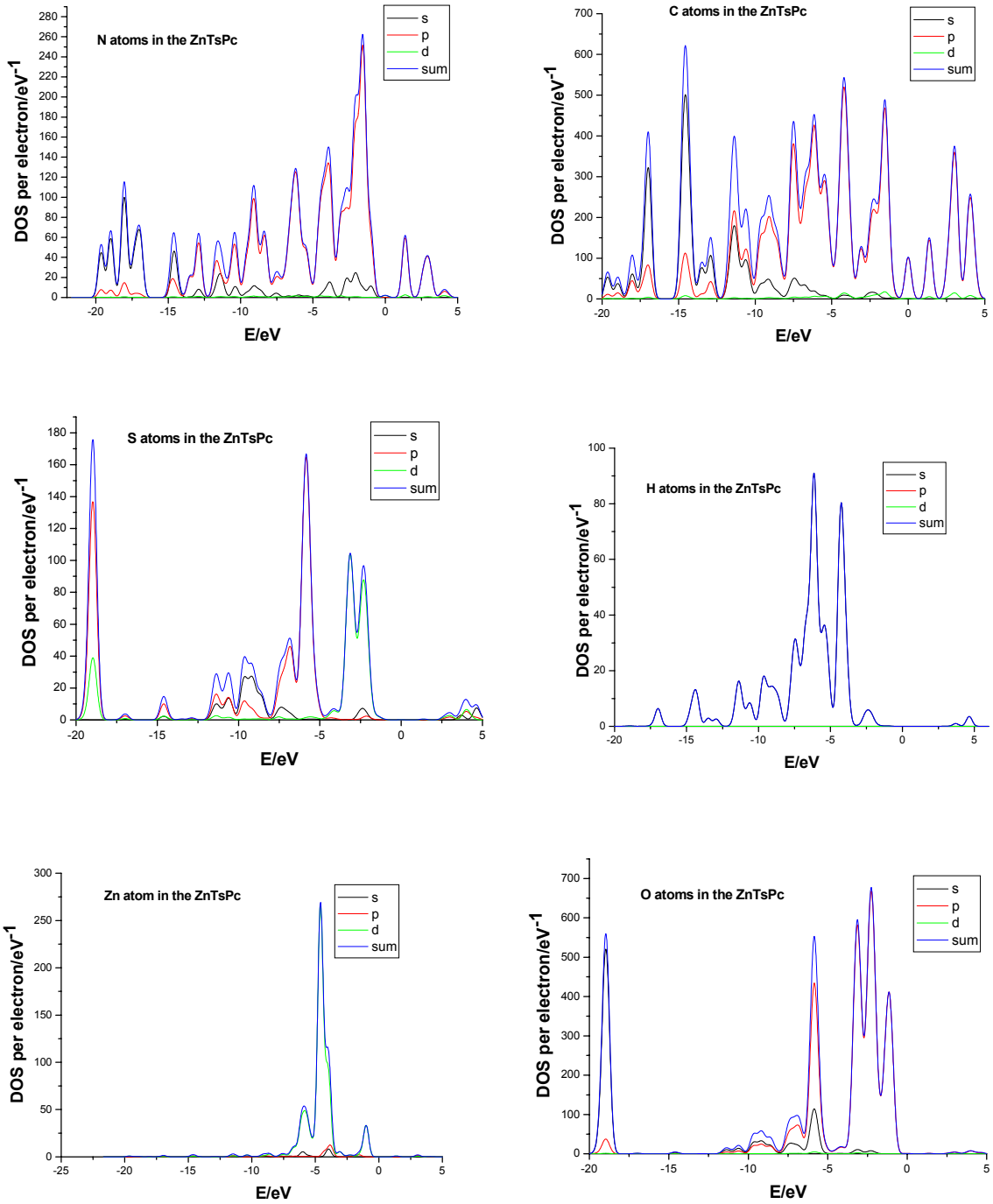

Fig. S9. PDOS of the atoms in ZnTSPc anions for the ZnTSPc/LDH system.

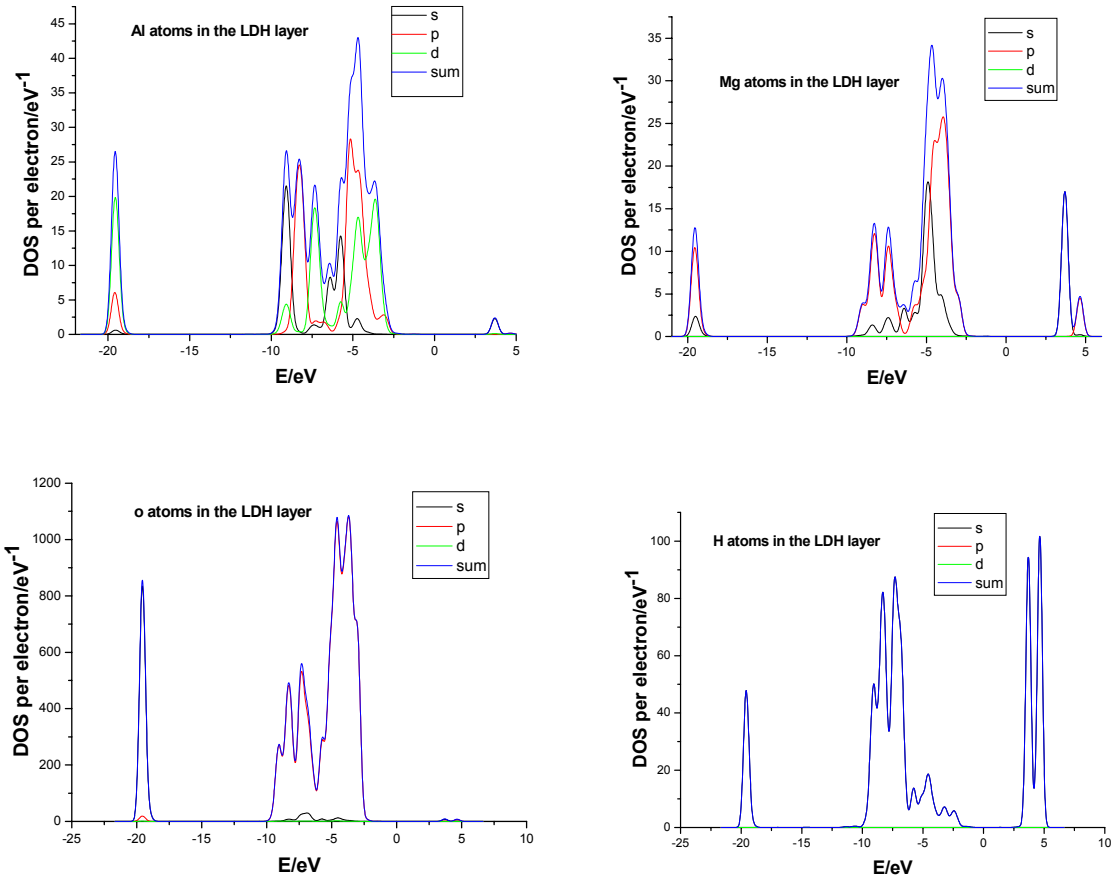

Fig. S10. PDOS of the atoms in LDH monolayer for the ZnTSPc/LDH system.

It can be observed from Fig. S9 and Fig. S10 that for the ZnTSPc/LDH system, the top of the valence band (TVB) is mainly located on the conjugated C atoms in ZnTSPc; the bottom of the conducting band (BCB) is mainly dominated by the C and N atoms in ZnTSPc. Around the Fermi level, the TDOS mainly consists of the 2p electrons of conjugated C atoms in ZnTSPc. The O 2p and Mg/Al 3s, H 1s orbitals from the LDH monolayers contribute to the TDOS below and above the TVB and BCB, respectively, with the gap of *ca*. 5.7 eV.

Reference:

[1] a) D. P. Yan, J. Lu, M. Wei, J. B. Han, J. Ma, F. Li, D. G. Evans, and X. Duan, *Angew. Chem. Int. Ed.* 2009, **48**, 3073; b) K. A. Carrado, J. E. Forman, R. E. Botto, and R. E. Winans *Chem. Mater.* 1993, **5**, 472.

[2] a) L. Mohanambe, and S. Vasudevan, *J. Phys. Chem. B* 2005, **109,** 15651. b) S. P. Newman, S. J. Williams, P. V. Coveney, and W. Jones, *J. Phys. Chem. B* 1998, **102,** 6710. c) E. Káfuňková, C Taviot-Guého, P. Bezdicka, Mariana Klementová, P. Kovár, P. Kubát, J. Mosinger, M. Pospıšil, and

K. Lang, *Chem. Mater.* 2010, **22**, 2481.

[3] a) B. Delley, *J. Chem. Phys.* 1990, **92,** 508. b) B. Delley, *J. Chem. Phys.* 2000, **113,** 7756. c) *Dmol3 Module, MS Modeling*, Version *2.2*; Accelrys Inc.: San, Diego, CA, 2003. d) J. R. Maple, M. -J. Hwang, T. P. Stockfisch, U. Dinur, M. Waldman, C. S. Ewig, and A. T. Hagler, *J. Comput. Chem.* 1994, **15,** 162. e) D. P. Yan, J. Lu, M. Wei, H. Li, J. Ma, F. Li, D. G. Evans, and X. Duan, *J. Phys. Chem. A* 2008, **112,** 7671; f) D. P. Yan, J. Lu, M. Wei, J. Ma, D. G. Evans, and X. Duan, *Phys. Chem. Chem. Phys.* 2009, **11**, 9200; g) J. P. Perdew, J. A. Chevary, S. H. Vosko, K. A. Jackson, M. R. Pederson, D. J. Singh, and C. Fiolhais, *Phys. Rev. B* 1992, **46,** 6671 ; h) S. H. Vosko, L. Wilk, and M. Nusair, Can. *J. Phys.* 1980, **58**, 1200.

[4] a) J. O. Morley, *J. Phys. Chem.* 1995, **99**, 1928. b) M.-S. Liao, and S. Scheiner, *J. Chem. Phys*. 2001, **114**, 9780.